EUROPEAN ORGANIZATION FOR NUCLEAR RESEARCH

CERN-PPE/94-221
December 13, 1994

# Observation of $\phi\phi$ production in the reaction $\bar{p}p \to 4K^{\pm}$ at 1.4 GeV/$c$ incident $\bar{p}$ momentum

the JETSET Collaboration:

L. Bertolotto[5,11], A. Buzzo[5], P.T. Debevec[6], D. Drijard[2], S. Easo[5,14], R.A. Eisenstein[6,15], W. Eyrich[3], T. Fearnley[2,16], H. Fischer[4], J. Franz[4], R. Geyer[3,7], N.H. Hamann[2,d], P.G. Harris[6,17], D.W. Hertzog[6], S.A. Hughes[6], A. Johansson[9], T. Johansson[9], R.T. Jones[2], K. Kilian[2], K. Kirsebom[5,10], A. Klett[4], H. Korsmo[8], M. Lo Vetere[5], M. Macrì[5], M. Marinelli[5], M. Moosburger[3], B. Mouëllic[2], W. Oelert[7], S. Ohlsson[2,13], A. Palano[1], S. Passaggio[5], J.-M. Perreau[2], M.G. Pia[5], S. Pomp[3,9], M. Price[2], P.E. Reimer[6], J. Ritter[6], E. Robutti[5], K. Röhrich[2,7], M. Rook[7], E. Rössle[4], A. Santroni[5], H. Schmitt[4], T. Sefzick[7], O. Steinkamp[7], F. Stinzing[3], B. Stugu[8,7,12], R. Tayloe[6], M. Tscheulin[4], H.J. Urban[4], H. Wirth[4], H. Zipse[4]

**Abstract**

The JETSET (PS202) experiment at CERN–LEAR searches for hadronic resonances by means of in-flight antiproton–proton annihilations in the reaction $\bar{p}p \to \phi\phi$. In order to obtain sufficient luminosity and good final-state mass resolution, this experiment uses an internal hydrogen-cluster jet target intersecting the LEAR antiproton beam. We report on the study of the reaction $\bar{p}p \to 4K^{\pm}$ at 1.4 GeV/$c$ incident $\bar{p}$ momentum, and we present the first experimental observation of a strong $\phi\phi$ signal in this reaction.

*(to be published in Physics Letters)*

[1] University of Bari and INFN, Bari, Italy
[2] CERN, Geneva, Switzerland
[3] University of Erlangen-Nürnberg, Erlangen, Germany
[4] University of Freiburg, Freiburg, Germany
[5] University of Genova and INFN, Genova, Italy
[6] University of Illinois, Urbana, Illinois, USA
[7] Institut für Kernphysik, Forschungszentrum Jülich, Jülich, Germany
[8] University of Oslo, Oslo, Norway
[9] Uppsala University, Uppsala, Sweden
[10] now at University of Århus, Århus, Denmark
[11] now at University of Edinburgh, Edinburgh, Scotland
[12] now at University of Bergen, Bergen, Norway
[13] now at CNRS, Lyon, France
[14] now at INFN, Perugia, Italy
[15] now at National Science Foundation, Washington DC, USA
[16] now at Niels Bohr Institute, University of Copenhagen, Copenhagen, Denmark
[17] now at University of Sussex, Sussex, England
[d] deceased

## 1 Introduction

Quantum Chromodynamics (QCD) is generally accepted to be the theory describing strong interactions. It is a peculiarity of QCD that, in addition to quarks, gluons too may play a structural role in hadronic states. This allows for various types of states that cannot be accounted for in Constituent Quark Models: glueballs, $(gg)$ or $(ggg)$; hybrids, $(\overline{q}qg)$; and multi-quark states, $(\overline{q}q\overline{q}q)$ or $(\overline{q}qqqq)$ for instance. The observation of such states would be a fundamental discovery [1].

Such unconventional forms of hadronic matter may appear experimentally as intermediate states in hadronic interactions. Particularly interesting are those reaction channels which do not have the same valence-quark flavours in the initial and final states. The production of hidden or open strangeness in $\overline{p}p$ annihilations constitutes a class of reactions which the JETSET (PS202) experiment at CERN–LEAR has chosen to study. The JETSET physics programme [2] focuses primarily on the investigation of the reaction $\overline{p}p \to \phi\phi$, where $\phi \to K^+K^-$ is the detected decay channel. At LEAR, this reaction can be studied from the $\phi\phi$ threshold ($\sqrt{s} = 2.04$ GeV) up to 2.43 GeV, corresponding to an incident antiproton momentum range of 0.866 to 2.0 GeV/$c$.

This process, with its disconnected quark lines, should be suppressed according to a strict interpretation of the OZI or quark-line rule [3] in which reactions with disconnected quark lines are forbidden. To such a rule, which is qualitative at best, there are known violations which result in cross-sections that are larger than expected. For example, violations can occur due to second-order two-step processes [4, 5], intermediate gluonic resonances [6], or inherent strange-quark content in the nucleon [7]. If the OZI rule were strictly enforced by nature, then the reaction $\bar{p}p \to \phi\phi$ could still proceed through the non-strange-quark component of the $\phi$ meson. This is implied by the slight departure from ideal mixing for the vector meson nonet [8]. This small departure can be used to determine a lower limit for the $\bar{p}p \to \phi\phi$ cross-section by comparison to the cross-section of the related reaction $\bar{p}p \to \omega\omega$. Unfortunately, only indirect evidence for the dominant decay channel of the latter reaction is reported in the literature [9], $\sigma(\bar{p}p \to 2\pi^+2\pi^-2\pi^0) \approx 7.8$ mb. For the related five-pion final state data which were measured directly by these authors, any specific two-body intermediate channel, like $\rho^0\omega$, constitutes only a few percent of the total cross-section. If we now assemble this information and make reasonable estimates, the contribution to the $\phi\phi$ total cross-section from this mixing can be expected to be on the order of 10 nb [10].

Very few experiments have conducted measurements of $\phi\phi$ production in $\overline{p}p$ annihilation. In an early bubble chamber experiment at ANL [11], six $\overline{p}p \to K^+K^-K^+K^-$ events were observed over a range of incident momenta from 1.6 to 2.2 GeV/$c$. The average cross-section for $\overline{p}p \to K^+K^-K^+K^-$ in this energy range was measured to be $(3.8 \pm 1.7)$ $\mu$b, with the conclusion (based on a single event) that the production cross-section for $\phi\phi$ was on the order of 2 $\mu$b. At a centre-of-mass energy $\sqrt{s}$ near 3 GeV, experiment R704 at CERN–ISR found $33 \pm 10$ $\bar{p}p \to \phi\phi$ events, yielding a cross-section of approximately 25 nb [12].

## 2 Detector

The JETSET experiment is located inside the LEAR machine and is shown schematically in Fig. 1. Its basic structure is a hydrogen-cluster jet target [13], of a density

$\rho = 4 \times 10^{12}$ atoms/cm$^2$, surrounded by a compact detector. The jet intersects the circulating antiproton beam at right angles in the horizontal plane. At a momentum of 1.4 GeV/$c$, the antiprotons stored in the machine have a revolution frequency $f = 3.17$ MHz. With a stored beam of $N_0 = 4 \times 10^{10}$ antiprotons, the luminosity is $\mathcal{L}_0 = \rho \cdot f \cdot N_0 = 5 \times 10^{29}$ cm$^{-2}$·s$^{-1}$.

One advantage of the jet-target technique applied to the LEAR storage ring is that the excellent beam-momentum resolution, $\Delta p/p \approx 10^{-3}$, results in a precise mass determination, $\Delta(\sqrt{s}) \approx 1$ MeV, for hadronic states that are directly formed in $\overline{p}p$ annihilations. In addition the high luminosity, which is one order of magnitude larger than that typically achieved in extracted-beam experiments, makes relatively rare processes like $\overline{p}p \to \phi\phi$ experimentally accessible.

Around the interaction volume the LEAR ring is equipped with an oval vacuum chamber (0.03 radiation lengths) having horizontal and vertical half-axes of 7.8 and 3.8 cm, respectively, and extending 31 cm downstream from the jet axis. These dimensions limit the geometrical acceptance of the detector to polar angles $\theta_{lab} > 7°$, with complete coverage of azimuthal angles only for $\theta_{lab} > 15°$.

The detector, which is non-magnetic, is composed of:

- 60 scintillation counters arranged around the beam pipe for triggering,
- 2400 single wire cylindrical drift chambers ("straws") for the tracking [14],
- 3700 silicon-pad counters arranged in two overlapping layers for the measurement of energy loss,
- 48 liquid threshold Čerenkov counters for fast pion rejection,
- multilayer scintillator hodoscope of 144-elements for triggering [15],
- 300 forward and 24 barrel electromagnetic shower counters [16], made of lead and scintillating fibres, for photon detection and rejection.

The online trigger was based on a charged-particle multiplicity of four, together with rejection of photons and fast pions. The results presented in this paper were derived from $5.5 \times 10^6$ such triggers collected during 60 hours of running at a $\bar{p}$ momentum of 1.4 GeV/$c$.

## 3 Analysis

The data analysis began with the reconstruction of four linear tracks which emerge from a common vertex within the interaction region. These four tracks were required to correspond one-to-one to hits in the trigger scintillators, which confines them all to the forward hemisphere and at least three of them to the region $\theta_{lab} \leq 45^{\mathrm{o}}$, defined with respect to the incident $\bar{p}$ direction. It was demanded that the four tracks, projected onto the transverse plane, not be confined to a half-plane, which would be inconsistent with momentum conservation for a four-particle final state. Any events with extra charged tracks, or with isolated neutral clusters in the barrel calorimeter exceeding 150 MeV of energy deposited, were rejected. There were $3.0 \times 10^4$ events that satisfied these criteria.

Since the detector is not equipped with a magnet, the momenta of the final-state particles are not measured directly, and must be inferred from 4-momentum conservation. Given an assumption on the masses of the four particles, the three equations obtained from 3-momentum conservation can be used to express the momenta of the particles as linear functions of one parameter, which we call $\mu$. The sum of the energies of the particles can

be expressed in terms of this parameter, $E_{final}(\mu)$, and one examines the function whose zeros satisfy energy conservation: $f(\mu) = E_{final}(\mu) - E_{initial}$. The second derivative of $f(\mu)$ is always positive, hence $f(\mu)$ has a single minimum which we call $\Delta E$, and the energy conservation equation $f(\mu) = 0$ has two solutions. Rejecting unphysical solutions, either complex in $\mu$ when $\Delta E > 0$, or real in $\mu$ but corresponding to negative momenta, one is left with cases with zero, one or two solutions. Owing to the observed accumulation of events near $\Delta E = 0$, the finite resolution of the detector demands that we accept a small violation of energy conservation. In the case $\Delta E \geq 0$ the solution was taken at the minimum of the function $f(\mu)$. Event candidates to the $\bar{p}p \to 4K^{\pm}$ reaction were selected by requiring $\Delta E \leq 20$ MeV. The resulting solutions were retained if all four calculated kaon momenta exceeded 200 MeV/$c$ (150 MeV/$c$ for $\theta > 45^0$), which is a practical limit stemming from energy loss and decay of slow particles.

Thus reconstructed, the kinematical solutions were tested for compatibility with the measured energy-loss in silicon detectors and the pulse-height information from the Čerenkov counters. The silicon $dE/dx$ compatibility was evaluated by forming the $\chi^2$ for each measurement, using the most-probable energy loss calculated from the kinematics as the expected value and using the width of the Landau peak as the r.m.s. To improve over the simple Gaussian approximation to the Landau distribution, a sharp cutoff was imposed on the low side of the distribution by assigning an infinite value for the $\chi^2$ if the measured value was less than 50% of the expected one. The $\chi^2$ values for each measurement were then added and the sum converted to a confidence level, which was required to be at least 5%. When two silicon hits were found on a single track, the smaller of the two measurements was used, in order to deplete the Landau tail. The Čerenkov counters, filled with liquid freon ($C_6F_{14}$, average refractive index 1.26), operated with a velocity threshold $\beta_0$=0.794. The Čerenkov effect produces a response $R(\beta)$ in photoelectrons that is monotonically increasing for $\beta \geq \beta_0$. This response function was used to calculate the expected Čerenkov response for each track. The expected and measured responses were compared on the basis of Poisson statistics. The resulting confidence levels for the four tracks were then combined to form an overall confidence level, which was required to be at least 5%. In the end the confidence levels from silicon and Čerenkov compatibility were combined to resolve the ambiguity arising when more than one kinematical solution passed the previous tests. In this case the solution having the highest combined probability was retained. There were 740 events that passed the particle-identification compatibility tests.

The admixture of background in this sample from final states other than $4K^{\pm}$ has been studied in the following way. For other four-prong final states with no neutrals, the selected events can be tested for compatibility with alternative mass hypotheses, and the best hypothesis chosen on the basis of the confidence level from particle identification. But for the $4\pi^{\pm}$ and the $2K^{\pm}2\pi^{\pm}$ final states, the near-threshold kinematics of the four-kaon reaction at 1.4 GeV/$c$ mean that there is practically no kinematical ambiguity between $4K^{\pm}$ and these channels. The $\bar{p}p\pi^+\pi^-$ final state is near to threshold at 1.4 GeV/$c$ and has a kinematical signature similar to $4K$. However the cross section for that reaction is on the order of 1 $\mu$b at 1.4 GeV/$c$ and so it is not an important source of background at this beam energy. In the $4K$ analysis procedure, all events that are accepted under the $4K$ hypothesis are also tested for compatibility with $\bar{p}p\pi^+\pi^-$, and ambiguous events are rejected. In addition to the 740 events in the above final sample, 8 additional ones were found which were compatibile with both $4K^{\pm}$ and $\bar{p}p\pi^+\pi^-$ at $CL \geq 5\%$ and so they were suppressed.

Monte Carlo studies of the final state $4K^{\pm}\pi^0$, where the $\pi^0$ goes undetected, show that an observable background from this channel can be ruled out, given the reasonable assumption that its cross section does not exceed 100 $\mu$b. Other channels containing one or more neutrals, however, are expected to enter at significant levels, based upon their known cross sections. Monte Carlo gives the following predictions for the $4K^{\pm}$ contamination at 1.4 GeV/$c$, $4\pi^{\pm}m\pi^0$ ($m \geq 0$) 6%, $2K^{\pm}2\pi^{\pm}m\pi^0$ 4%, and $K^+\bar{K}^0 2\pi^-\pi^+$ + $c.c.$ 2%. The Monte Carlo simulation used a uniform Lorentz-invariant phase space weight and so these numbers can be taken only as order-of-magnitude estimates. A more quantitative estimate of the non-$4K^{\pm}$ background in the final sample is obtained from the $\Delta E$ distribution, as described later. By far the most important means by which background channels are rejected is the restriction of all four charged tracks to $\theta_{lab} < 65^o$. The veto of isolated neutral clusters in the barrel region and particle identification constraints play an important role in rejecting reactions with neutrals in the final state.

In order to study the background still present in the selected data sample and to measure the total four-kaon yield, we made use of the $\Delta E$ distribution, suspending the requirement on $\Delta E \leq 20$ MeV. Fig. 2 shows this distribution for four-kaon event candidates before (Fig. 2a) and after (Figs. 2b-d) having applied the particle identification cuts. In particular, Fig. 2b shows the effect of applying particle identification by using the $dE/dx$ in the silicon detectors only. Fig. 2c on the other hand shows the effect produced on the $\Delta$E distribution by applying the particle identification using the Čerenkov counters only. Finally Fig. 2d shows the effect of applying both types of identification. The latter distribution shows a clean enhancement around $\Delta E = 0$.

A properly reconstructed four-kaon event must have $\Delta E \leq 0$ (within measurement errors) in order to possess at least one kinematical solution which satisfies energy conservation. Monte Carlo simulations show that the $\Delta E$ distribution for $4K^{\pm}$ final states is sharply peaked towards $\Delta E = 0$, with a tail that extends out as far as $\Delta E = -50$ MeV. To predict the four-kaon $\Delta E$ distribution expected for real data, Monte Carlo events from the reactions $\bar{p}p \rightarrow \phi\phi$ and $\bar{p}p \rightarrow 4K^{\pm}$ (phase space) have been generated using a detailed detector simulation based upon GEANT [17]. These events were then analysed as if they were real data. There was no significant difference between the shape of the Monte Carlo $\Delta E$ distributions for the two reactions. We fit the $\Delta E$ distribution of the real data to a superposition of this shape plus a smooth background. The background was parameterized as [18] $(E - E_0)^{\alpha} \times e^{(-\beta E - \gamma E^2)}$ (where $E_0, \alpha, \beta$ and $\gamma$ are free parameters). Adjusting the shape of the background and allowing the central peak to vary only in height, a good description of the real data is obtained, as can be seen in Fig. 2d, where the dashed line represents the fitted background.

Finally, if the condition $\Delta E \leq 20$ MeV is brought back again, the fit to the $\Delta E$ distribution can be used to estimate the fraction of the events passing this cut that belong to the reaction $\bar{p}p \rightarrow 4K^{\pm}$ (resonance channels included). This procedure yields $615 \pm 46(stat.) \pm 123(syst.)$ $4K^{\pm}$ out of the 740 final events. An event-by-event separation is not possible by this procedure. In assigning a systematic error to this result, we took into account the fact that the shape of the $\Delta E$ distribution for four-kaon events has some dependence on the kaon angular distributions in the final state, which for the physical process are not necessarily isotropic as was assumed in the Monte Carlo generation. The systematic error quoted above is the maximum variation in the $4K^{\pm}$ yield estimate that can be obtained by distorting the shape of the background function, under the assumption

that it goes to zero with the data on the left of the distribution and joins smoothly to the shape of the data at the right in Fig. 2d.

For the selected four-kaon event candidates we show in Fig. 3a the Goldhaber plot of invariant mass pairs. Since the charges of the kaons were not measured, all three possible $m(K_1K_2), m(K_3K_4)$ combinations are entered in the plot for each event. There is a clear enhancement in the $\phi\phi$ region. The accumulation visible near the diagonal edge of phase space is the combinatoric reflection of the $\phi\phi$ peak. Fig. 3b shows the $m(KK)$ effective mass distribution. Fig. 3c shows the $K_1K_2$ effective mass distribution when the opposite combination $(K_3K_4)$ lies in the $\phi$ band $(1.0 \leq m(KK) \leq 1.04$ GeV$/c^2)$. A clean $\phi$ signal with little background can be seen. A fit performed to this mass spectrum using a Breit-Wigner plus a smooth background [18] (see Fig. 3c) gives $m = 1019.2 \pm 0.4$ MeV$/c^2$, in excellent agreement with the PDG mass [8] of the $\phi(1020)$, and a full width $\Gamma = 14.5 \pm 0.9$ MeV$/c^2$ arising mainly from our tracking resolution [19]. This width may be compared with $\Gamma = 13.0 \pm 0.2$ MeV$/c^2$ obtained from the analysis of Monte Carlo data.

In order to estimate the number of $\phi\phi$ events in this distribution, we make use of the channel likelihood technique [20]. For the $\phi$ resonance lineshape, the fit used a Breit-Wigner with a width taken from Monte Carlo, and assumed isotropic production and decay angular distributions. The method has been tested by Monte Carlo simulations in a large variety of signal-to-background conditions and in each case the method consistently reproduced the input parameters to within statistical errors. Three hypotheses are considered in the fit: $\phi\phi$, $\phi K^+K^-$ and $4K^\pm$ phase space. Monte Carlo studies have shown that events from background reactions, when reconstructed under the four-kaon mass hypothesis, form a broad continuum in the four-kaon mass plots. Thus the background which extends under the peak in the $\Delta E$ plot (see the dashed curve in Fig. 2d) is indistinguishable from the four-kaon phase space by the channel likelihood fit. The fit gives as $\phi\phi$ and $\phi K^+K^-$ contributions $(57.2 \pm 2.9)\%$ and $(2.0 \pm 5.0)\%$ respectively, the latter consistent with zero. Suppressing the $\phi K^+K^-$ hypothesis and fitting with $\phi\phi$ and phase-space only, we obtain $(57.6 \pm 2.7)\%$ as the fraction of $\phi\phi$ signal in this sample, corresponding to $426 \pm 25$ events. To display the quality of the fit we superimpose in Figs. 3b and 3c, as shaded histograms, the corresponding $m(KK)$ distributions which are found by the fit to belong to phase space. We observe that no $\phi$ signal has been left in the fitted non-resonant background contribution.

Fig. 3d shows the distribution of $\cos\theta_{cm}$ for events in the region of the $\phi\phi$ peak in the Goldhaber plot, where $\theta_{cm}$ is the angle formed by one $\phi$ with respect to the incident $\bar{p}$ beam in the centre-of-mass system. The superimposed histogram in the figure is obtained from an isotropic Monte Carlo simulation, normalized to the data. The loss of acceptance at small $\theta_{cm}$ reflects the loss of forward-going kaons in the vacuum pipe.

The acceptance was calculated by generating Monte Carlo events according to the reaction under study, and simulating the detector response using GEANT. Since the $\phi$ production angle and polarization distributions are unknown, the production and decay angular distributions were generated isotropically in the respective centre-of-mass systems. The non-resonant kaons were generated according to Lorentz-invariant phase space. The resulting record of hits was subjected to the online trigger conditions and submitted to the standard analysis chain in the same way as the real data. The ratio of final signal to the number of events originally generated gives the acceptance. This procedure gives an overall value of the acceptance of 1.85% for the $\phi\phi$ reaction, of 0.98% for the $\phi K^+K^-$,

and of 1.16% for the $4K^{\pm}$ reaction at 1.4 GeV/$c$ incident $\bar{p}$ momentum, where only the charged-kaon decay of the $\phi$ was allowed in the simulation.

The luminosity was measured using elastic $\bar{p}p$ scattering. A coincidence between opposing pairs of pixels in the forward hodoscope measured the elastic $\bar{p}p$ scattering rate for symmetric kinematics. The yield of such events was corrected for trigger and analysis efficiencies. The trigger acceptance ($\approx$ 10 msr) and the analysis efficiency ($\approx$ 90%) were estimated by Monte Carlo simulations, in a similar way as described above. The luminosity was then determined by comparison with published $\bar{p}p$ cross-sections [21]. A check of the luminosity measurement was performed by using the method of beam attenuation [22]. In this method, the rate of decrease in the intensity of the stored beam, along with the known total $\bar{p}p$ cross-section, is used to estimate the effective thickness of the target. During periods of smooth LEAR operation, luminosities from the two methods were in agreement within 10%. The integrated luminosity is 25.4 nb$^{-1}$ $\pm$ 1%($stat.$) $\pm$ 15%($syst.$), including only the time during which the data acquisition was ready to accept the next trigger. The 15% systematic error includes 5% uncertainty for the previous measurement of the elastic scattering cross-section [21] used for normalization. The luminosity calculated by the beam decay method was not used in obtaining this figure because that method is sensitive to parameters of the machine that were not monitored.

A reaction with a topological signature very similar to $\bar{p}p \rightarrow 4K^{\pm}$ is $\bar{p}p \rightarrow \bar{p}p\pi^+\pi^-$. The cross-section for this process is small at 1.4 GeV/$c$, but at higher momenta it dominates $\bar{p}p \rightarrow 4K^{\pm}$ in our event sample, and therefore can be used to test our estimates for the systematic errors. Data taken at 1.9 GeV/$c$ under similar trigger conditions to those used at 1.4 GeV/$c$ have been analysed, with the four-kaon mass hypothesis replaced by the one appropriate to $\bar{p}p\pi^+\pi^-$. After correction for acceptance we measure a cross-section of

$$\sigma(\bar{p}p \rightarrow \bar{p}p\pi^+\pi^-) = 165 \pm 4(stat.) \pm 17(syst.) \quad \mu b$$

at 1.9 GeV/$c$ incident momentum. This value has to be compared with extrapolated cross-sections at 1.9 GeV/$c$ of 180 $\pm$ 30$\mu$b [23] and 250 $\pm$ 40$\mu$b [24]. The agreement is an independent confirmation of our luminosity measurement, within the stated errors.

## 4 Results

From the analysis of our data we report the cross-sections shown in Table 1. Those involving the $\phi$ have been corrected for unseen decay modes ($B.R.(\phi \rightarrow K^+K^-) = 0.491 \pm 0.008$) [8]. It was viewed as unlikely that the non-$4K$ background in the final sample would exhibit a narrow structure at the $\phi$ resonance, hidden under the peak in the mass plot in such a way that the resonance lineshape (in comparison with that from Monte Carlo) would not show a noticeable distortion. Under this assumption, the presence of this background has little influence on the $\phi\phi$ yield from the channel-likelihood fit, which is sensitive mainly to reproducing the size of the peak. What is left after the resonant part is removed is a sum of background plus those $4K^{\pm}$ channels other than $\phi\phi$ or $\phi K^+K^-$, called here *non-resonant* $4K^{\pm}$. The non-resonant $4K^{\pm}$ cross-section in Table 1 is calculated after subtraction of the background. It includes in an effective way the contributions from two-kaon resonances other than the $\phi(1020)$, whose tails extend into the allowed phase-space shown in Fig. 3(a-c), such as the $f_0(980)$, $f_2(1270)$, $f_0(1300)$ and $a_2(1320)$.

The systematic errors reported for the cross-sections in Table 1 include contributions

| reaction channel | fraction (%) ± stat. err. | yield ± stat. err. | acceptance (%) | cross-section ($\mu$b) | stat. error | syst. error |
|---|---|---|---|---|---|---|
| $\phi\phi$ | $57.2 \pm 2.9$ | $423 \pm 27$ | 1.85 | 3.73 | $\pm 0.24$ | $\pm 0.81$ |
| $\phi K^+K^-$ | $2.0 \pm 5.0$ | $15 \pm 37$ | 0.98 | $< 0.67$ (90% c.l.) | | |
| non-resonant | $40.8 \pm 4.7$ | $302 \pm 36$ | | | | |
| non-res. $4K^\pm$ | | $177 \pm 36$ | 1.16 | 0.60 | $\pm 0.12$ | $\pm 0.44$ |

Table 1: Final results for the four-kaon final-state reactions from $\overline{p}p$ annihilation in flight. The partial cross-sections (see text), which are corrected for unseen decay modes of the $\phi$, are calculated using an integrated luminosity of $25.4 \pm 3.8$ nb$^{-1}$ and a total yield of $740 \pm 27$ events. The results for the non-resonant component are given in two steps, the first before correction for non-four-kaon background and the second following the correction. The errors on the luminosity and acceptance are systematic in nature; their statistical errors are much smaller and are neglected. The systematic error on the final cross-sections includes contributions from the fit fraction (5%), luminosity (15%), acceptance (15%), and background subtraction (non-resonant $4K^\pm$ only, see text), summed in quadrature.

from four sources: channel likelihood fit procedure, acceptance, luminosity, and background subtraction. The systematics in the fit procedure reflect the dependence of the result on the empirical function that is used to describe the $\phi$ lineshape. The results reported here were obtained by fixing the $\phi$ mass at its PDG value and setting the $\phi$ width according to a fit to reconstructed Monte Carlo data (see Fig. 3c). By varying the width within the limits permitted by the data, and observing the accompanying shift in the fit results, we estimate a systematic error of 5% on the fit procedure. The most important unknown factor in the acceptance is the efficiency of the online trigger. This we estimate to be $\pm 15\%$, to be reduced in the future by studies of triggers taken under minimum-biased conditions. The 15% error stated above on the luminosity is entirely systematic in nature; the statistical errors are less than 1%. The background subtraction is currently assigned a $\pm 100\%$ error, to be reduced by further studies. It does not apply to the channels containing one or more $\phi$'s. Since these four errors come from independent sources, they are uncorrelated and so they are combined in quadrature to obtain an estimate for the overall systematic error, shown in Table 1. It is important to point out that this large systematic error is mainly an uncertainty on the absolute value of the luminosity and the acceptance, and cancels to a large extent when ratios of cross-sections are taken, *e.g.* when one measures the shape of the excitation function as a function of $\sqrt{s}$.

In interpreting these results, it is important to keep in mind the limited acceptance in the centre-of-mass production angle (see Fig. 3d) of this measurement. Because it is impossible to make a meaningful extrapolation into the forward region based upon events confined to the region $\theta_{cm} > 45^{\circ}$, we do not report this result as a total cross-section. Rather it is presented as a partial cross-section integrated over the accepted solid angle $\Omega$ and multiplied by the factor $4\pi/\Omega$. The last factor is included to enable the simple interpretation of a total cross-section under the assumption of isotropic production, and enables a comparison with the previous estimates for the total cross-section. More precisely,

$$\sigma = \frac{Y}{\mathcal{L}\mathcal{A}} \tag{1}$$

where $Y$ is the yield for the channel in question, $\mathcal{L}$ is the luminosity, and $A$ is the average

acceptance for isotropic and unpolarized production.

The goal of the Jetset experiment is to investigate the possibility of resonance formation in $\overline{p}p$ annihilations to final states containing strange mesons, and in particular $\phi\phi$. The experiment has performed the first real measurement of the cross-section for this important channel, and has found a strong $\phi\phi$ signal that dominates the $4K^{\pm}$ final state at 1.4 GeV/$c$ incident $\bar{p}$ momentum. Data of similar quality have been taken with the Jetset apparatus in a set of about 50 momentum values spread out over the range from 1.18 to 2.0 GeV/$c$. With these data it will be possible to map out the excitation function for $\phi\phi$ production with a statistical precision of 5-10%, depending on the point, and a relative point-to-point systematic error on the same order of magnitude. Although the limited acceptance of the experimental setup prevents us from making a precise statement about the total cross-section, it is clear from our measurement at 1.4 GeV/$c$ that it exceeds expectations based upon the OZI rule by two orders of magnitude. At this point it is unknown how much, if any, of this excess is related to the formation of s-channel resonances. This question can only be answered by experiment. If one or more resonances do play a role then the determination of the mass, width, and quantum numbers of these mesonic states would be important towards the clarification of the meson spectrum in the mass region above 2 GeV/$c^2$.

## 5 Acknowledgements

The Collaboration owes much to the technicians and support staff at the participating institutes, without whose dedicated efforts the construction of the experimental apparatus would not have been accomplished. We thank the teams of the CERN Antiproton Complex, in particular the LEAR staff, for their excellent cooperation during the installation and the running of the experiment. R.K. Bock, J. Kirkby and M. Poulet are thanked for their contributions during the early phase of the experiment. This work has been supported in part by CERN, the German Bundesministerium für Forschung und Technologie, the Italian Istituto Nazionale di Fisica Nucleare, the Swedish Natural Science Research Council, the Norwegian Natural Science Research Council, and the United States National Science Foundation, under contract NSF PHY 89-21146.

## References


[1] For reviews see:
K. Königsmann, Proceedings of the XI Int. Conf. "Physics in Collisions", Colmar (France), June 20-22 1991, pp. 355-377;
T.H. Burnett and S.R. Sharpe, Ann. Rev. Nucl. Part. Sci. **40** (1990) 327;
K. Peters, Nucl. Phys. **A558** (1993) 93c.

[2] N.H. Hamann et al., *Proc. International School on Physics with Low-Energy Antiprotons (4th Course: Medium-Energy Antiprotons and the Quark–Gluon Structure of Hadrons)*, Erice, 1990, eds. R. Landua, J.–M. Richard and R. Klapisch (Plenum Press, New York, 1991) 165.

[3] S. Okubo, Phys. Lett. **5** (1963) 165,
G. Zweig, CERN report TH-412 (1964),
J. Iizuka, Prog. Theor. Phys. Suppl. **37/38** (1966) 21.

[4] Y. Lu, B.S. Zou, and M.P. Locher, Z. Phys. **A345** (1993) 207.

[5] V. Mull, The $\bar{N}N \to \pi\pi$ and $\bar{N}N \to \phi\phi$ reactions with hadronic models, presented at NAN'93, Moscow, Russia, 13-18 Sept. 1993,
"The $\bar{p}p \to \phi\phi$ reaction as a two-step process involving antihyperon-hyperon intermediate states", submitted to Phys. Lett. B.

[6] S.J. Lindenbaum, Comm. Nucl. Phys. **13** (1984) 285.

[7] J. Ellis, E. Gabathuler, and M. Karliner, Phys. Lett. **B217** (1989) 173.

[8] Review of particles properties, Phys. Rev. **D45** (1992) 1.

[9] J. Clayton et al., Nucl. Phys. **B30** (1971) 605,
R.A. Donald et al., Nucl. Phys. **B11** (1969) 551.

[10] The $\phi\phi$ cross-section contribution from the admixture of non-strange quarks in the $\phi$ meson can be estimated from the relation $\sigma(\bar{p}p \to \phi\phi) \approx \tan^4(\theta_{ideal} - \theta_V)\sigma(\bar{p}p \to \omega\omega)$ where $\theta_{ideal} = 35.5^{\mathrm{o}}$ is the ideal mixing angle and $\theta_V = 36^{\mathrm{o}} - 39^{\mathrm{o}}$ represents the range of determined values for the vector meson nonet. A value for $\sigma(\bar{p}p \to \omega\omega)$ can be taken as a fraction of the measured $\sigma(\bar{p}p \to 2\pi^+2\pi^-2\pi^0)$ result. We estimate this fraction to be less than 10%.

[11] J. Davidson et al., Phys. Rev. **D9** (1974) 77.

[12] C. Baglin et al., Phys. Lett. **B231** (1989) 557.

[13] M. Macrì, GAS Jet Internal Target in CERN 84/15 (1984) 469,
M. DiCapua et al., CERN/Jetset 89-22 (1989).

[14] N.H. Hamann et al., Nucl. Instr. and Meth. **A346** (1994) 57.

[15] M. Dahmen et al., Nucl. Instr. and Meth. **A348** (1994) 97.

[16] D.W. Hertzog et al., Nucl. Instr. and Meth. **A294** (1990) 446.

[17] R. Brun et al., GEANT3, CERN Report DD/EE/84-1 (1987).

[18] P. Granet et al., Nucl. Phys. **B140** (1978) 389.

[19] The width of the $\phi$ peak in the reconstructed $4K^{\pm}$ sample is mainly determined by the uncertainty on the track directions which are supplied as input to the kinematical reconstruction. Tracking resolution is approximately $\pm 2^{\mathrm{o}}$ r.m.s., limited by multiple-scattering in the material inside the tracker, except for $\pm 3^{\mathrm{o}}$ on the polar angle of the barrel track, which is limited by the charge-division resolution of the barrel tracker. Less important contributions to the total $\phi$ width include the momentum spread of the beam and the intrinsic width of the $\phi$ meson ($\Gamma = 4.4$ MeV/$c^2$).

[20] P.E. Condon and P. Cowell, Phys. Rev. **D9** (1974) 2558.

[21] V. Flaminio et al., CERN-HERA 84-01, 17 April 1984.

[22] C. Evangelista et al., CERN/SPSLC 92-42, SPSLC M501, 10 August, 1992
[23] J. Lys et al., Phys. Rev. **D7** (1973) 610.
[24] P.S. Eastman et al., Nucl. Phys. **B51** (1973) 29.

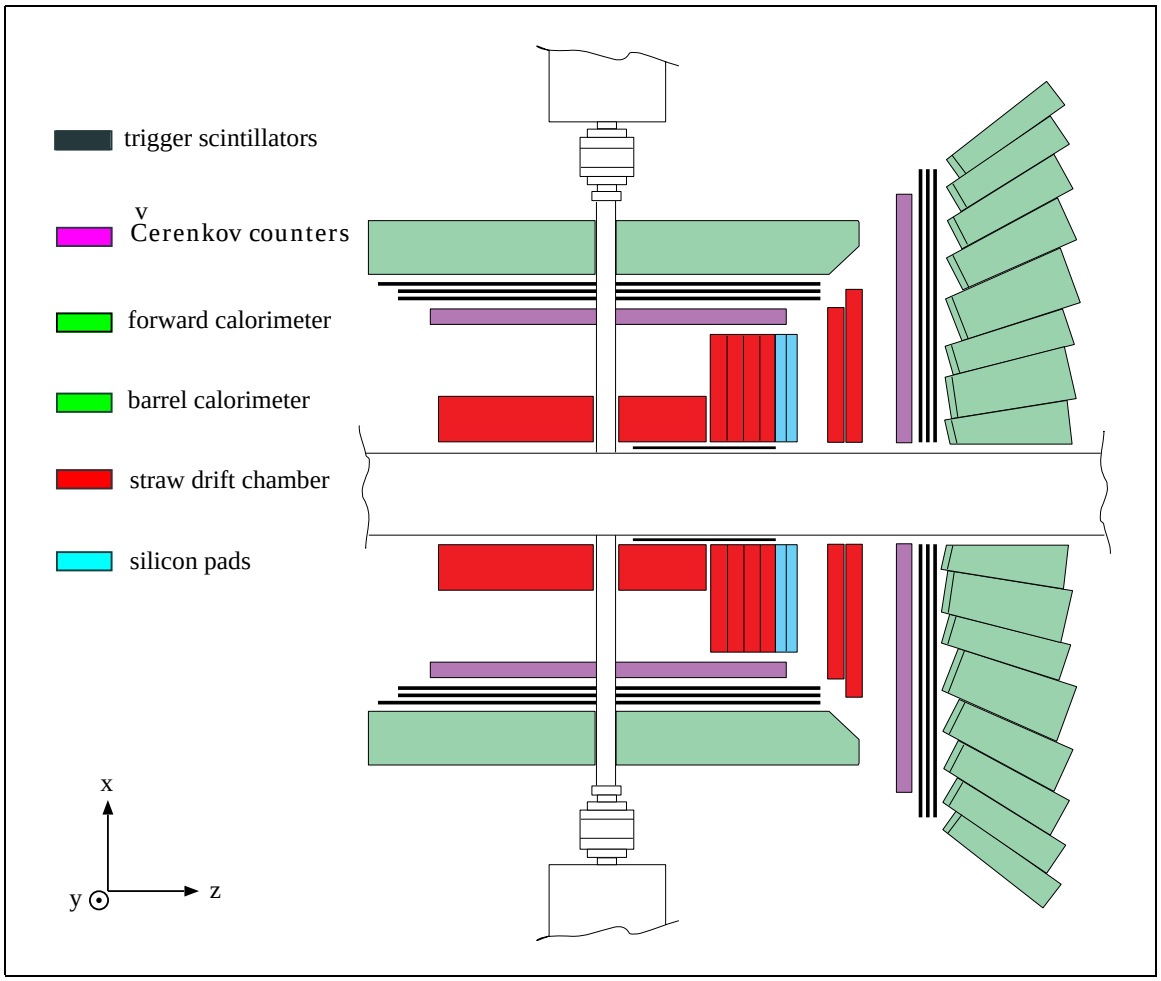


Figure 1: Layout of JETSET/PS202 experiment, showing the major detector components.

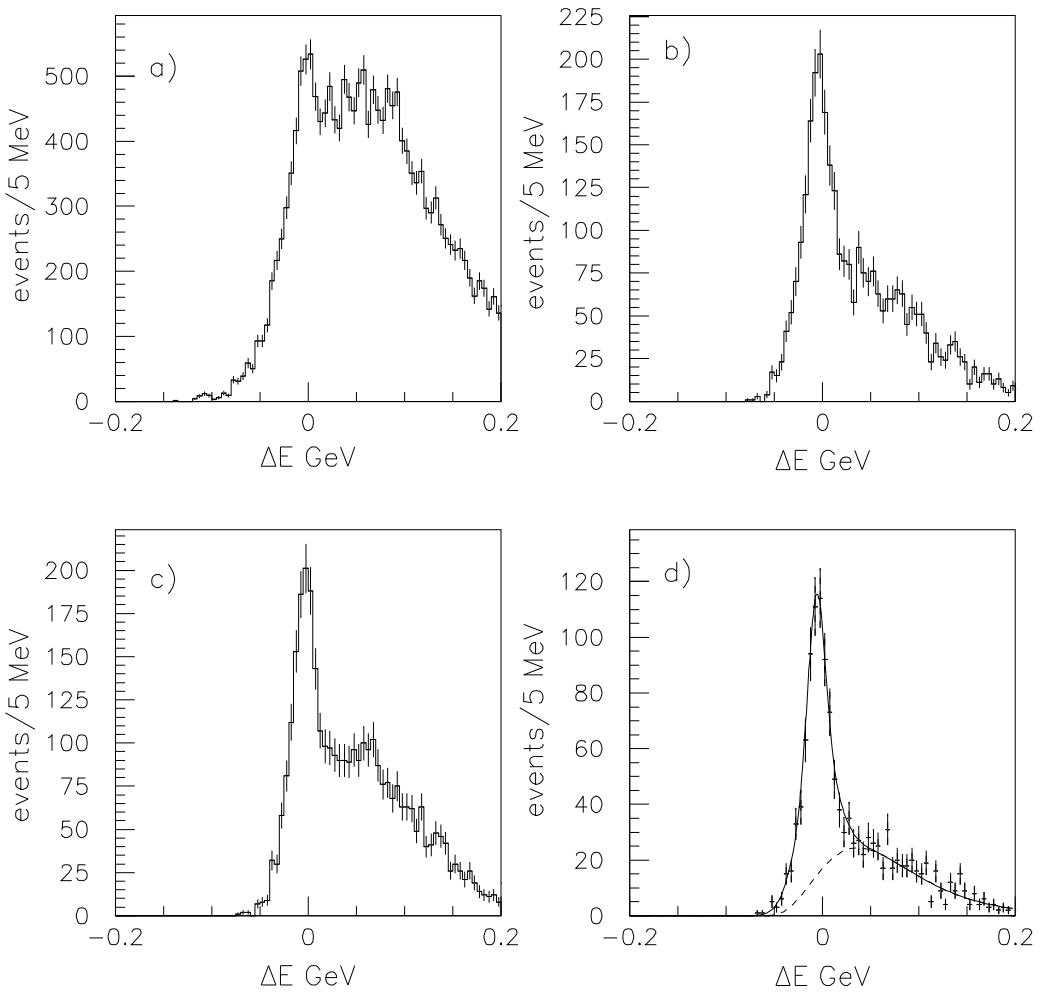


Figure 2: $\Delta E$ distribution for event candidates of the reaction $\bar{p}p \to 4K$ at 1.4 GeV/$c$ incident $\bar{p}$ momentum, for (a) four-prong events prior to particle identification; (b) after having applied particle identification from the silicon detectors alone; (c) after having applied particle identification from the Čerenkov counters alone; (d) after both particle identification cuts. The solid curve in (d) is the result of a fit using the $\Delta E$ peak derived from four-kaon Monte Carlo plus a smooth background (dashed curve).

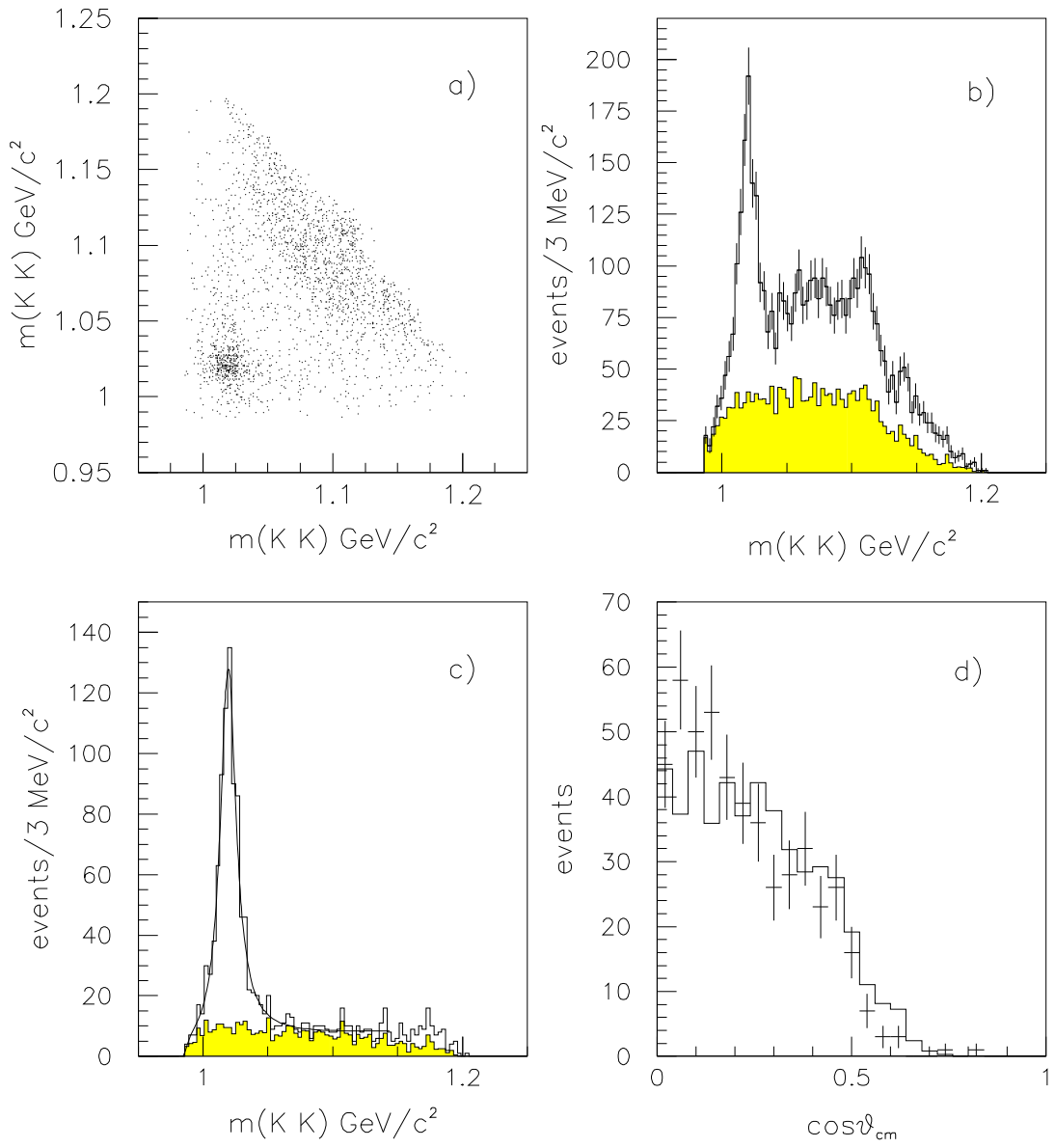


Figure 3: (a) Goldhaber scatter plot of $m(K_3K_4)$ vs. $m(K_1K_2)$ at 1.4 GeV/$c$ incident $\bar{p}$ momentum, with three entries per event due to charge ambiguities; (b) two-kaon invariant mass distribution, with six entries per event due to charge ambiguities; (c) distribution of two-kaon invariant mass $m(K_1K_2)$ when the opposite combination $m(K_3K_4)$ falls in the $\phi$ band, with up to four entries per event; (d) $cos\theta_{cm}$ distribution for the events that lie within a circle of radius 20 MeV/$c^2$ centered on the $\phi\phi$ peak in (a). The shaded histograms in (b) and (c) represent the portion of the data which is allocated to non-resonant channels by the channel-likelihood fit (see text). The solid curve in (c) is a fit to the spectrum using a Breit-Wigner plus a smooth (Granet) background. In (d) the points with error bars represent the data and the solid histogram is from Monte Carlo simulation of the $\phi\phi$ channel, assuming isotropic angular distributions.